

# Spin correlations in the two-leg antiferromagnetic ladder in a magnetic field

T. Hikihara

*Department of Earth and Space Science, Graduate School of Science, Osaka University,  
Toyonaka, Osaka 560-0043, Japan*

A. Furusaki

*Yukawa Institute for Theoretical Physics, Kyoto University, Kyoto 606-8502, Japan  
(November 20, 2000)*

We study the ground-state spin correlations in the gapless incommensurate regime of a  $S = 1/2$   $XXZ$  chain and a two-leg antiferromagnetic ladder under a magnetic field, in which the gapless excitations form a Tomonaga-Luttinger (TL) liquid. We calculate numerically the two-spin correlation functions and the local magnetization in the two models using the density-matrix renormalization-group method. By fitting the numerical results for an open  $XXZ$  chain of 100 spins to correlation functions of a Gaussian model, we determine the TL-liquid parameter  $K$  and the amplitudes of the correlation functions. The value of  $K$  estimated from the fits is in excellent agreement with the exact value obtained from the Bethe ansatz. We apply the same method to the open ladder consisting of 200 spins and determine the dependence of  $K$  on the magnetization  $M$ . The  $K$ - $M$  relation changes drastically depending on the ratio of the coupling constants in the leg and rung directions. We also discuss implications of these results to experiments on the nuclear spin relaxation rate  $1/T_1$  and dynamical spin structure factors.

75.10.Jm, 75.40.Cx, 75.50.Ee, 75.40.Mg

## I. INTRODUCTION

Spin ladder systems have been studied extensively over the past decade.<sup>1</sup> There are reasons why the ladders have attracted so much attention. Firstly, they naturally interpolate one- and two-dimensional systems and may provide some hints to better understand the high-temperature superconductivity which occurs in square lattice  $\text{CuO}_2$  planes. Secondly, spin ladders themselves have interesting physics and deserve thorough investigation in their own right. One of their most surprising properties is that low-energy physics of spin ladders depends drastically on the number of legs. Spin- $1/2$  antiferromagnetic (AF) ladders, for example, have a finite gap in the spin excitation spectrum in the even-leg case, whereas they have no gap in the odd-leg case. The ground state of an even-leg ladder is a spin singlet and its properties can be understood from the short-range resonating-valence-bond picture.<sup>2</sup> This spin-gap behavior has been observed experimentally on  $S = 1/2$  two-leg ladder compounds,<sup>3,4</sup> such as  $\text{SrCu}_2\text{O}_3$  and  $\text{Cu}_2(\text{C}_5\text{H}_{12}\text{N}_2)_2\text{Cl}_4$ .

A gapless phase can appear in even-leg ladders when an external field  $h$  is applied. If the field  $h$  is larger than a critical field  $h_{c1}$ , which is equal to the spin gap, and if it is smaller than the saturation field  $h_{c2}$ , then the ground state has a nonzero magnetization  $M$  and the energy gap between the ground state and the first-excited states vanishes. The gapless mode has been shown to be described as a Tomonaga-Luttinger (TL) liquid both in the strong- and weak-coupling limit,<sup>5-7</sup> where the coupling in the rung-direction  $J_\perp$  is much larger or much smaller than the one in the leg-direction  $J_\parallel$ , respectively. However, the  $M$  dependence of the TL-liquid param-

eter  $K$ , which governs the spin correlations in long wave length, has been obtained analytically only in the strong-coupling limit and it remains as a nontrivial problem to determine  $K$  for general  $J_\perp/J_\parallel$ . In the gapless phase the system shows incommensurate spin correlations since the Fermi wavenumber of Jordan-Wigner fermions is shifted from  $\pi/2$  in the presence of the magnetic field which acts as a chemical potential for the fermions. The wavenumber  $Q$  characterizing the incommensurability of the gapless mode varies continuously as  $h$  increases. This gapless incommensurate (IC) phase is in fact in the same universality class as the one-dimensional  $S = 1/2$   $XXZ$  model in a magnetic field, as we will see.

In this paper, we study low-energy properties of the  $S = 1/2$  two-leg AF ladder in the gapless IC regime for broad range of  $J_\perp/J_\parallel$ . We show that the system is a TL liquid for arbitrary  $J_\perp/J_\parallel$  and determine the  $M$  dependence of  $K$  numerically. To this end, we compute numerically the ground-state spin-correlation functions and the local magnetization in the open ladders using the density-matrix renormalization-group (DMRG) method<sup>9,10</sup> and extract the TL-liquid parameter by fitting the data to correlation functions obtained from the Abelian bosonization. This method was applied in our previous work<sup>8</sup> to the  $S = 1/2$   $XXZ$  chain at  $h = 0$  and proved to be effective in determining both the TL-liquid parameter and amplitudes of correlation functions. In order to demonstrate the validity of the analysis in the gapless IC phase, we first apply it to the  $S = 1/2$   $XXZ$  chain for  $h > 0$ . The model is exactly solvable by the Bethe ansatz and the TL-liquid parameter  $K$  can be calculated for arbitrary value of  $M$ . It thus provides a good test ground to check accuracy of our method. We find

that  $K$  estimated from the DMRG data is in excellent agreement with the exact calculation. We then apply the same method to the two-leg ladders in a magnetic field. Our numerical data of correlation functions are fitted well for broad range of  $J_{\perp}/J_{\parallel}$  to the formulas based on the bosonization approach, confirming that the gapless modes are in fact in the universality class of a TL liquid for arbitrary  $J_{\perp}/J_{\parallel}$ . The  $M$  dependence of  $K$  obtained in the large  $J_{\perp}/J_{\parallel}$  limit agrees with the analytic result obtained through mapping to the  $XXZ$  chain. In this limit  $K$  is less than 1 for  $0 < M < 1$ . As  $J_{\perp}/J_{\parallel}$  decreases,  $K$  increases and become larger than 1 for intermediate values of  $M$ . Our numerical result indicates that  $K$  takes a universal value 1 for any  $J_{\perp}/J_{\parallel}$  in the limits  $M \rightarrow 0$  and  $M \rightarrow 1$ .

The plan of the paper is as follows. We first review the Abelian bosonization approach to the  $S = 1/2$   $XXZ$  chain under a magnetic field in Sec. II A. The formulas of the spin correlations and the local magnetization in finite open chains are presented. In Sec. II B, we show numerical data for the  $XXZ$  chain of  $L = 100$  sites obtained from the DMRG calculation and fit the data to the functions given in Sec. II A. In Sec. III A, we briefly review some relevant results of the previous analytic studies on the two-leg ladders in the strong- and weak-coupling limits. The DMRG data and the results of fitting on the open ladders with  $L = 200$  sites are shown in Sec. III B. The  $M$  dependence of  $K$  for various values of  $J_{\perp}/J_{\parallel}$  is obtained. Its implications to NMR and neutron scattering experiments are briefly mentioned. Finally, our results are summarized in Sec. IV.

## II. $XXZ$ CHAIN

### A. Bosonization approach

In this section, we consider spin-1/2  $XXZ$  chains with open ends in a magnetic field  $h$ . The Hamiltonian is

$$\mathcal{H}_{\text{ch}} = \mathcal{H}_0 + \mathcal{H}_h \quad (1)$$

with

$$\begin{aligned} \mathcal{H}_0 &= J \sum_{l=1}^{L-1} (\mathbf{S}_l, \mathbf{S}_{l+1})_{\Delta}, \\ \mathcal{H}_h &= -h \sum_{l=1}^L S_l^z, \end{aligned}$$

where  $\mathbf{S}_l$  are  $S = 1/2$  spin operators and  $(\mathbf{S}_l, \mathbf{S}_{l'})_{\Delta} = S_l^x S_{l'}^x + S_l^y S_{l'}^y + \Delta S_l^z S_{l'}^z$ . We assume the system size  $L$  to be even throughout this paper and treat only the case where  $J > 0$  and  $0 \leq \Delta \leq 1$ . We note that the Hamiltonian (1) for  $-1 < \Delta \leq 1$  can be solved exactly by Bethe ansatz for arbitrary values of  $h$ .<sup>11–13</sup>

We use the standard Abelian bosonization techniques to analyze spin-spin correlation functions at zero temperature. We basically follow the scheme presented in Ref. 14 and generalize it to the case of open chains in magnetic fields. The bosonization formulas in the absence of magnetic fields are reported in Ref. 8.

The low-energy dynamics of  $XXZ$  chains is described by the Gaussian model,<sup>12</sup>

$$\tilde{\mathcal{H}}_{\text{ch}} = \frac{v}{2} \int_0^{L+1} dx \left[ \left( \frac{d\phi}{dx} \right)^2 + \left( \frac{d\tilde{\phi}}{dx} \right)^2 \right], \quad (2)$$

where  $v$  is the spin-wave velocity. The continuous variable  $x$  is identified with the site index  $l$  under the assumption that the lattice spacing equals unity. The bosonic fields  $\phi(x)$  and  $\tilde{\phi}(x)$  obey the commutation relation  $[\phi(x), \tilde{\phi}(y)] = -i\Theta(x - y)$ , where  $\Theta(x)$  is the step function. The spin operators in the original Hamiltonian (1) are related to the bosonic fields by the relations,

$$S_l^z = \frac{1}{2\pi R} \frac{d\phi}{dx} + a(-1)^l \sin\left(\frac{\phi(l)}{R}\right), \quad (3)$$

$$S_l^- = \exp[-i2\pi R\tilde{\phi}(l)] \left[ b \sin\left(\frac{\phi(l)}{R}\right) + c(-1)^l \right], \quad (4)$$

with  $a$ ,  $b$ , and  $c$  being real constants. The parameter  $R$  determines the exponents of correlation functions. We also introduce the TL-liquid parameter  $K$  by  $K = 1/(4\pi R^2)$ ;  $K = 1$  in the  $XY$  case ( $\Delta = 0$ ), and  $K = 1/2$  in the Heisenberg case ( $\Delta = 1$ ) at  $h = 0$ . From Eq. (4),  $S_l^x$  is written as

$$S_l^x = c(-1)^l \cos[2\pi R\tilde{\phi}(l)] - ib \sin[2\pi R\tilde{\phi}(l)] \sin\left(\frac{\phi(l)}{R}\right). \quad (5)$$

The second term with the coefficient  $ib$  is Hermitian due to the commutation relation  $[\phi(l), \tilde{\phi}(l)] = -i/2$ . The open boundary conditions are translated to the boundary conditions on the bosonic fields at the two phantom sites  $l = 0$  and  $l = L+1$ :<sup>14</sup>  $\phi(0) = 0$  and  $\phi(L+1) = 2\pi RLM_{\text{ch}}$ , where  $M_{\text{ch}}$  is the magnetization per site,

$$M_{\text{ch}} = \frac{1}{L} \sum_{l=1}^L S_l^z. \quad (6)$$

The total magnetization  $LM_{\text{ch}}$  is an integer for even  $L$ . These boundary conditions lead to the mode expansion,

$$\phi(x) = \frac{x}{L+1} \phi_0 + \sum_{n=1}^{\infty} \frac{\sin(q_n x)}{\sqrt{\pi n}} (a_n + a_n^{\dagger}), \quad (7)$$

$$\tilde{\phi}(x) = \tilde{\phi}_0 + i \sum_{n=1}^{\infty} \frac{\cos(q_n x)}{\sqrt{\pi n}} (a_n - a_n^{\dagger}), \quad (8)$$

where  $q_n = \pi n/(L+1)$ ,  $[\tilde{\phi}_0, \phi_0] = i$ , and  $a_m$  are boson annihilation operators obeying  $[a_m, a_n^{\dagger}] = \delta_{m,n}$ . Note that

the commutation relation between  $\phi(x)$  and  $\tilde{\phi}(y)$  mentioned above is satisfied. The lowest energy state  $|M_{\text{ch}}\rangle$  in the subspace in which the magnetization per spin is  $M_{\text{ch}}$  is a vacuum of  $a_n$

$$a_n|M_{\text{ch}}\rangle = 0 \quad (9)$$

and an eigenstate of  $\phi_0$

$$\phi_0|M_{\text{ch}}\rangle = 2\pi RLM_{\text{ch}}|M_{\text{ch}}\rangle. \quad (10)$$

We may regard  $\tilde{\phi}_0$  as a coordinate variable along a fictitious ring of radius  $1/2\pi R$  and take  $\phi_0 = -id/d\phi_0$  to be

$$\begin{aligned} \langle S_l^x S_{l'}^x \rangle &\equiv X(l, l'; q) \\ &= \frac{f_{\eta/2}(2l)f_{\eta/2}(2l')}{f_{\eta}(l-l')f_{\eta}(l+l')} \left[ \frac{c^2}{2}(-1)^{l-l'} + \frac{bc}{2}\text{sgn}(l-l') \left( \frac{(-1)^l \cos(ql')}{f_{1/2\eta}(2l')} - \frac{(-1)^{l'} \cos(ql)}{f_{1/2\eta}(2l)} \right) \right. \\ &\quad \left. - \frac{b^2}{4f_{1/2\eta}(2l)f_{1/2\eta}(2l')} \left( \cos[q(l+l')] \frac{f_{1/\eta}(l-l')}{f_{1/\eta}(l+l')} + \cos[q(l-l')] \frac{f_{1/\eta}(l+l')}{f_{1/\eta}(l-l')} \right) \right], \quad (11) \end{aligned}$$

$$\begin{aligned} \langle S_l^z S_{l'}^z \rangle &\equiv Z(l, l'; q) \\ &= \frac{q}{2\pi} \left( \frac{q}{2\pi} + a \frac{(-1)^l \sin(ql)}{f_{1/2\eta}(2l)} + a \frac{(-1)^{l'} \sin(ql')}{f_{1/2\eta}(2l')} \right) - \frac{1}{4\pi^2\eta} \left( \frac{1}{f_2(l-l')} + \frac{1}{f_2(l+l')} \right) \\ &\quad + \frac{a^2}{2} \frac{(-1)^{l+l'}}{f_{1/2\eta}(2l)f_{1/2\eta}(2l')} \left( \cos[q(l-l')] \frac{f_{1/\eta}(l+l')}{f_{1/\eta}(l-l')} - \cos[q(l+l')] \frac{f_{1/\eta}(l-l')}{f_{1/\eta}(l+l')} \right) \\ &\quad + \frac{a}{2\pi\eta} \left( \frac{(-1)^l \cos(ql)}{f_{1/2\eta}(2l)} [g(l+l') + g(l-l')] + \frac{(-1)^{l'} \cos(ql')}{f_{1/2\eta}(2l')} [g(l+l') - g(l-l')] \right), \quad (12) \end{aligned}$$

$$\langle S_l^z \rangle \equiv z(l; q) = \frac{q}{2\pi} + a \frac{(-1)^l \sin(ql)}{f_{1/2\eta}(2l)}, \quad (13)$$

where

$$\eta = 2\pi R^2 = \frac{1}{2K}, \quad (14)$$

$$f_{\alpha}(x) = \left[ \frac{2(L+1)}{\pi} \sin \left( \frac{\pi|x|}{2(L+1)} \right) \right]^{\alpha}, \quad (15)$$

$$g(x) = \frac{\pi}{2(L+1)} \cot \left( \frac{\pi x}{2(L+1)} \right). \quad (16)$$

The wavenumber  $q$ , characterizing the IC character of the spin correlations in a magnetic field, is related to  $M_{\text{ch}}$  by

$$q = \frac{2\pi M_{\text{ch}}L}{L+1}. \quad (17)$$

The factor  $L/(L+1)$  appears as a result of the open boundary conditions. Under the periodic boundary conditions  $q$  should be simply equal to  $2\pi M_{\text{ch}}$ , because the first term in Eq. (7) is  $\phi_0 x/L$  in this case. This term must be  $\phi_0 x/(L+1)$  in the open-boundary case in order for  $\phi(x)$  and  $\tilde{\phi}(x)$  to satisfy the commutation relation in the interval  $[0, L+1]$ . We emphasize that Eqs. (12) and (13) reproduce the exact results for the XY chain when

its momentum conjugate. The state  $|M_{\text{ch}}\rangle$  is then proportional to  $\exp(i2\pi RLM_{\text{ch}}\phi_0)$ . The bosonization formulas (3) and (4) represent only the leading contributions. In the next order  $S_l^-$  has a term of the form  $(-1)^l \exp[-2\pi i R \tilde{\phi}(l)] \cos[2\phi(l)/R]$ . We will, however, ignore this contribution because it yields only subleading corrections that disappear quickly for large  $|l-l'|$ .

Using Eqs. (3)–(10), one can evaluate the two-spin correlation functions  $\langle S_l^{\alpha} S_{l'}^{\alpha} \rangle$  ( $\alpha = x, z$ ) and the local magnetization  $\langle S_l^z \rangle$  in open chains, where  $\langle \dots \rangle$  denotes the expectation value in the state  $|M_{\text{ch}}\rangle$ . Brief account of their derivation is given in Appendix. Here we present the final results:

$\eta = 1/2$  and  $a = -1/\pi$ . As is well known, the XXZ spin chain is equivalent to a model of spinless fermions with nearest-neighbor interaction. In this model,  $S_l^z$  is none but the fermion density, and the oscillating term in Eq. (13) corresponds to the Friedel oscillations near the open ends.<sup>15–18</sup>

In the thermodynamic limit ( $L \rightarrow \infty$ ) with  $|l-L/2| \ll L$  and  $|l'-L/2| \ll L$ , the spin correlations have the asymptotic forms

$$\langle S_l^x S_{l'}^x \rangle = A_x \frac{(-1)^{l-l'}}{|l-l'|^{\eta}} - \hat{A}_x \frac{\cos[q(l-l')]}{|l-l'|^{\eta+1/\eta}}, \quad (18)$$

$$\begin{aligned} \langle S_l^z S_{l'}^z \rangle &= M_{\text{ch}}^2 + A_z (-1)^{l-l'} \frac{\cos[q(l-l')]}{|l-l'|^{1/\eta}} \\ &\quad - \frac{1}{4\pi^2\eta |l-l'|^2}, \quad (19) \end{aligned}$$

where the correlation amplitudes  $A_x$ ,  $\hat{A}_x$ , and  $A_z$  are related to the numerical constants  $a$ ,  $b$ , and  $c$  by  $A_x = c^2/2$ ,  $\hat{A}_x = b^2/4$ , and  $A_z = a^2/2$ . We can therefore estimate the TL-liquid parameter and the correlation amplitudes

in the thermodynamic limit by extracting the fitting parameters  $R$ ,  $a$ ,  $b$ , and  $c$  from the numerical data on a finite system with use of Eqs. (11), (12), and (13). At the same time, the TL-liquid parameter  $K$  can be calculated exactly for any  $M_{\text{ch}}$  by solving an integral equation obtained from the Bethe ansatz.<sup>19,20</sup> We will compare our estimates of  $K$  obtained from the fitting procedure with the Bethe ansatz results in the next subsection.

## B. Numerical results

Using the DMRG method,<sup>9,10</sup> we computed the two-spin correlation functions  $\langle S_l^\alpha S_{l'}^\alpha \rangle$  ( $\alpha = x, z$ ) and the local magnetization  $\langle S_l^z \rangle$  in the  $L = 100$  open chains. The two-point functions were calculated for  $l = r_0 - r/2$  and  $l' = r_0 + r/2$ , where  $r_0 = L/2$  for even  $r$  and  $r_0 = (L+1)/2$  for odd  $r$ . The calculation was performed for each lowest-energy state of  $\mathcal{H}_0$  in the subspace of various values of  $M_{\text{ch}}$ . We employed the finite system algorithm of improved version.<sup>21</sup> The maximum number of kept states  $m$  is 100. We estimate the numerical error due to the truncation of the Hilbert space from the difference between the data with  $m = 100$  and those with  $m = 70$ . The estimated errors for  $\langle S_l^x S_{l'}^x \rangle$ ,  $\langle S_l^z S_{l'}^z \rangle$ , and  $\langle S_l^z \rangle$  are, at largest, of order  $10^{-5}$ ,  $10^{-6}$ , and  $10^{-6}$ , respectively.

In Fig. 1, we show the spin correlations  $\langle S_l^\alpha S_{l'}^\alpha \rangle$  ( $\alpha = x, z$ ) and the local magnetization  $\langle S_l^z \rangle$  at  $\Delta = 0.5$  for three different values of  $M_{\text{ch}}$ . The DMRG data are shown by open symbols whose sizes are larger than the truncation error mentioned above. Taking  $R$ ,  $a$ ,  $b$ , and  $c$  as fitting parameters, we fit the numerical data to Eqs. (11)–(13). The results of the fitting using the DMRG data of

$\langle S_l^\alpha S_{l'}^\alpha \rangle$  for  $10 \leq r \leq 90$  and of  $\langle S_l^z \rangle$  for  $1 \leq l \leq 100$  are also plotted in the figure by the small solid symbols. One can see that the fits are in excellent agreement with the DMRG data, proving the validity of the bosonization formulas (11)–(13).

For various values of  $M_{\text{ch}}$  and  $\Delta$ , we determined the parameters  $R$ ,  $a$ ,  $b$ , and  $c$  by the fitting procedure. In doing so we used numerical data of several ranges,  $10 \leq r \leq 80$ ,  $10 \leq r \leq 90$ ,  $20 \leq r \leq 80$ , and  $20 \leq r \leq 90$  for the two-spin correlation functions and  $1 \leq l \leq 100$  and  $10 \leq l \leq 90$  for the local magnetization. We take the mean and the variance of the fitting parameters obtained for the different ranges of  $r$  and  $l$  as the estimated value and the error of the estimates, respectively. The TL-liquid parameter  $K \equiv 1/(4\pi R^2)$  estimated from the numerical data of  $\langle S_l^x S_{l'}^x \rangle$  is plotted as a function of  $M_{\text{ch}}$  in Fig. 2. The exact values obtained from the Bethe ansatz method<sup>19,20</sup> are also shown as dotted lines. The agreement is excellent. We also estimated  $K$  from the fitting of  $\langle S_l^z S_{l'}^z \rangle$  and  $\langle S_l^z \rangle$  and obtained similar results as Fig. 2. We found, however, that the estimates from the last two correlators show some deviations from the Bethe ansatz results when  $K$  is small. We do not exactly know why they deviate. One possible reason might be the effect of the leading irrelevant operator neglected in the Gaussian model that becomes marginal at  $K = 1/2$ . In the  $XY$  regime of our interest, spins have stronger correlations in the  $S^x$  and  $S^y$  components than in  $S^z$ , and thus we may expect that  $\langle S_l^x S_{l'}^x \rangle$  should give us most reliable estimates.

For the correlation amplitudes  $A_x$  and  $A_z$ , Lukyanov and Zamolodchikov conjectured the exact formulas which are valid at  $h = 0$ ,<sup>22,23</sup>

$$A_x^{\text{LZ}} = \frac{1}{8(1-\eta)^2} \left[ \frac{\Gamma(\frac{\eta}{2(1-\eta)})}{2\sqrt{\pi}\Gamma(\frac{1}{2(1-\eta)})} \right]^\eta \exp \left[ - \int_0^\infty \frac{dt}{t} \left( \frac{\sinh(\eta t)}{\sinh(t) \cosh[(1-\eta)t]} - \eta e^{-2t} \right) \right], \quad (20)$$

$$A_z^{\text{L}} = \frac{2}{\pi^2} \left[ \frac{\Gamma(\frac{\eta}{2(1-\eta)})}{2\sqrt{\pi}\Gamma(\frac{1}{2(1-\eta)})} \right]^{1/\eta} \exp \left[ \int_0^\infty \frac{dt}{t} \left( \frac{\sinh[(2\eta-1)t]}{\sinh(\eta t) \cosh[(1-\eta)t]} - \frac{2\eta-1}{\eta} e^{-2t} \right) \right], \quad (21)$$

where  $\Gamma(x)$  is the Gamma function. Equations (20) and (21) have been confirmed numerically.<sup>8,23</sup> In Table I, we give our estimates of the correlation amplitudes  $A_x = c^2/2$  and  $A_z = a^2/2$  obtained from the fitting of  $\langle S_l^x S_{l'}^x \rangle$  and  $\langle S_l^z \rangle$  for  $0 < M_{\text{ch}} < 0.5$ , together with the exact values (20) and (21) at  $M_{\text{ch}} = 0$ .<sup>24</sup> As can be seen in Table I (a),  $A_x$  decreases monotonically from the value given by Eq. (20) to zero as  $M_{\text{ch}}$  increases from 0 to  $1/2$ . Thus,  $A_x$  depends not only on  $K$  but also on  $M_{\text{ch}}$ . (See, for example, the data for  $\Delta = 0$  where  $K$  takes a constant value 1 for any  $M_{\text{ch}}$ .) When  $M_{\text{ch}}$  approaches  $1/2$ , where  $K \rightarrow 1$ ,  $A_x$  seems to go to zero linearly for any  $\Delta$ . This can be easily understood once we consider one-magnon contribution to the correlation function. On the other hand,  $A_z$  decreases monotonically from the number given by Eq. (21) to the uni-

versal value  $A_z = 1/(2\pi^2) \simeq 0.05066$  as  $M_{\text{ch}}$  increases from 0 to  $1/2$ .<sup>25</sup> An exception is the case  $\Delta = 0$ , where  $A_z = 1/(2\pi^2)$  for any  $M_{\text{ch}}$ . The convergence of  $A_z$  to  $1/(2\pi^2)$  at  $M_{\text{ch}} \rightarrow 1/2$  is consistent with the fact that the correlator  $\langle S_l^z S_{l'}^z \rangle$  must take a constant value  $1/4$  at  $M_{\text{ch}} = 1/2$ . The right-hand side of Eq. (19) equals  $M_{\text{ch}}^2$  when  $\eta = 1/2$ ,  $q = \pi$ , and  $A_z = 1/(2\pi^2)$ .

## III. TWO-LEG AF LADDER

Encouraged by the success in the last section, we study the two-leg AF ladders in a magnetic field using the same method. We begin with a brief review of the analytic results on the ladder in the strong- and weak-coupling limits.

## A. Review of Analytic Results

The Hamiltonian of the open two-leg ladder studied in this section is given by

$$\mathcal{H} = J_{\parallel} \sum_{\mu=1,2} \sum_{l=1}^{L-1} (\mathbf{S}_{\mu,l}, \mathbf{S}_{\mu,l+1})_{\Delta} + J_{\perp} \sum_{l=1}^L (\mathbf{S}_{1,l}, \mathbf{S}_{2,l})_{\Delta} - h \sum_{\mu=1,2} \sum_{l=1}^L S_{\mu,l}^z. \quad (22)$$

The anisotropy  $\Delta$  is introduced for generality. We assume that the coupling in the leg- and rung-direction,  $J_{\parallel}$  and  $J_{\perp}$ , are positive (antiferromagnetic). The spin ladder has an excitation gap in weak magnetic fields  $h < h_{c1}$ . We concentrate on the ladder in the gapless IC regime, i.e., in the case  $h_{c1} \leq h \leq h_{c2}$ . We denote the ratio  $J_{\perp}/J_{\parallel}$  by  $j$  hereafter.

We begin with the strong-coupling limit ( $j \gg 1$ ), for which a simple intuitive picture is available. It is known that the system in this limit can be mapped to an effective  $S = 1/2$   $XXZ$  chain,<sup>7,26,27</sup> as we explain below. Let us first assume  $J_{\parallel} = 0$ . In this case, an eigenstate of  $\mathcal{H}$  is written as a direct product of rung states. At each rung two spins  $\mathbf{S}_{1,l}$  and  $\mathbf{S}_{2,l}$  are either in a singlet state  $|s_l\rangle = (|\uparrow\downarrow\rangle - |\downarrow\uparrow\rangle)/\sqrt{2}$  or in one of the triplet states,  $|t_l^+\rangle = |\uparrow\uparrow\rangle$ ,  $|t_l^0\rangle = (|\uparrow\downarrow\rangle + |\downarrow\uparrow\rangle)/\sqrt{2}$ , and  $|t_l^-\rangle = |\downarrow\downarrow\rangle$ . When  $h$  is small, the ground state consists of a product of the singlet rungs. As the field  $h$  increases, the energy of the state  $|t_l^+\rangle$  becomes lower, and at  $h = J_{\perp}(1+\Delta)/2$ , the state degenerates with  $|s_l\rangle$ . We can thus analyze the low-energy properties of the system for  $h \simeq J_{\perp}(1+\Delta)/2$  by retaining only the two lowest-energy states  $|s_l\rangle$  and  $|t_l^+\rangle$  for each rung. We may regard the two states as “down” and “up” states of an effective  $S = 1/2$  spin,

$$\tilde{S}_l^x = -\frac{1}{\sqrt{2}}(S_{1,l}^x - S_{2,l}^x), \quad \tilde{S}_l^y = -\frac{1}{\sqrt{2}}(S_{1,l}^y - S_{2,l}^y), \quad (23)$$

$$\tilde{S}_l^z = S_{1,l}^z + S_{2,l}^z - \frac{1}{2}. \quad (24)$$

The effective spins  $\tilde{\mathbf{S}}_l$  are the only low-energy degrees of freedom, and their dynamics is governed by

$$\begin{aligned} \tilde{\mathcal{H}} = & J_{\parallel} \sum_{l=1}^{L-1} (\tilde{\mathbf{S}}_l, \tilde{\mathbf{S}}_{l+1})_{\Delta/2} - \frac{\Delta}{4} J_{\parallel} (\tilde{S}_1^z + \tilde{S}_L^z) \\ & - \left( h - \frac{1+\Delta}{2} J_{\perp} - \frac{\Delta}{2} J_{\parallel} \right) \sum_{l=1}^L \tilde{S}_l^z + \text{const.} \end{aligned} \quad (25)$$

This mapping is derived in lowest order in  $J_{\parallel}/J_{\perp}$  and valid for the entire IC region of  $0 < M < 1$ , where  $M$  is magnetization per rung

$$M = \frac{1}{L} \sum_{l=1}^L (S_{1,l}^z + S_{2,l}^z). \quad (26)$$

Note that the anisotropy of the effective  $S = 1/2$   $XXZ$  chain is a half of the anisotropy of the original ladder,  $\Delta/2$ . Besides the bulk effective magnetic field  $h - (1+\Delta)J_{\perp}/2 - \Delta J_{\parallel}/2$ , there is an additional field  $-\Delta J_{\parallel}/4$  applied only to the boundary spins  $\tilde{S}_1^z$  and  $\tilde{S}_L^z$ . It induces oscillating magnetization near the boundaries superposed on the Friedel oscillation which is already present at any  $M \neq 0$  without the boundary field. The effect of the boundary field may be cancelled by adding an extra term

$$\mathcal{H}' = h' \sum_{\mu=1,2} (S_{\mu,1}^z + S_{\mu,L}^z) \quad (27)$$

to the original ladder Hamiltonian (22), where  $h' = \Delta J_{\parallel}/4$  for  $j \gg 1$ . Now we define

$$\mathbf{S}_{0,l} = \mathbf{S}_{1,l} + \mathbf{S}_{2,l}, \quad (28)$$

$$\mathbf{S}_{\pi,l} = \mathbf{S}_{1,l} - \mathbf{S}_{2,l}. \quad (29)$$

From the mapping explained above, we conclude that the two-spin correlations  $\langle S_{\pi,l}^x S_{\pi,l'}^x \rangle$  and  $\langle S_{0,l}^z S_{0,l'}^z \rangle$  and the local magnetization  $\langle S_{0,l}^z \rangle$  in the open ladder  $\mathcal{H} + \mathcal{H}'$  in the limit  $j \gg 1$  are given by the corresponding correlators in the  $XXZ$  chain. We thus obtain

$$\langle S_{\pi,l}^x S_{\pi,l'}^x \rangle = 2X(l, l'; Q), \quad (30)$$

$$\begin{aligned} \langle S_{0,l}^z S_{0,l'}^z \rangle &= \left\langle \left( \frac{1}{2} + \tilde{S}_l^z \right) \left( \frac{1}{2} + \tilde{S}_{l'}^z \right) \right\rangle \\ &= \frac{1}{4} + \frac{1}{2} [z(l; Q) + z(l'; Q)] + Z(l, l'; Q), \end{aligned} \quad (31)$$

$$\langle S_{0,l}^z \rangle = \frac{1}{2} + z(l, Q), \quad (32)$$

where the wavenumber is

$$Q = \frac{2\pi L}{L+1} \left( M - \frac{1}{2} \right). \quad (33)$$

In the limit  $L \rightarrow \infty$  the two-spin correlation functions reduce to

$$\begin{aligned} \langle S_{\pi,l}^x S_{\pi,l'}^x \rangle &= 2A_x \frac{(-1)^{l-l'}}{|l-l'|^{1/2K}} \\ &\quad - 2\hat{A}_x (-1)^{l-l'} \frac{\cos[2\pi M(l-l')]}{|l-l'|^{2K+(1/2K)}}, \end{aligned} \quad (34)$$

$$\begin{aligned} \langle S_{0,l}^z S_{0,l'}^z \rangle &= M^2 - \frac{1}{4\pi^2 \eta |l-l'|^2} \\ &\quad + A_z \frac{\cos[2\pi M(l-l')]}{|l-l'|^{2K}}. \end{aligned} \quad (35)$$

Note that they can be obtained from Eqs. (18) and (19) by replacing  $q$  and  $M_{\text{ch}}$  with  $2\pi(M-1/2)$  and  $M$ , respectively. On the other hand, the correlations  $\langle S_{0,l}^x S_{0,l'}^x \rangle$  and  $\langle S_{\pi,l}^z S_{\pi,l'}^z \rangle$  decay exponentially because  $S_{0,l}^x$  and  $S_{\pi,l}^z$  always create the high-energy rung states  $|t_l^0\rangle$  and  $|t_l^-\rangle$  as a virtual excited state.

Next, we consider the opposite case, the weak-coupling limit ( $j \ll 1$ ). The system in this limit has been investigated with the Abelian bosonization method.<sup>5–7</sup> In these studies, two chains are first bosonized independently, and then the interchain coupling  $J_{\perp}$  is treated perturbatively.<sup>28</sup> Four bosonic fields  $\phi_{\pm}(x)$  and  $\tilde{\phi}_{\pm}(x)$  are introduced, where  $\phi_{+}$  and  $\tilde{\phi}_{+}$  ( $\phi_{-}$  and  $\tilde{\phi}_{-}$ ) are the symmetric (antisymmetric) combinations of bosonic fields of each chain. All the fields are massive<sup>28</sup> when  $h < h_{c1}$ . In the IC regime of  $h_{c1} \leq h \leq h_{c2}$ , on the other hand, the fields  $\phi_{+}$  and  $\tilde{\phi}_{+}$  become massless while the fields  $\phi_{-}$  and  $\tilde{\phi}_{-}$  remain massive. The low-energy effective Hamiltonian for the gapless modes has the same form as that of the  $S = 1/2$   $XXZ$  chain, Eq. (2). Furthermore, the spin correlation functions  $\langle S_{\pi,l}^x S_{\pi,l'}^x \rangle$  and  $\langle S_{0,l}^z S_{0,l'}^z \rangle$  have the same  $r$  dependence as in the strong-coupling limit (but with different values of  $K$ ,  $a$ ,  $b$ , and  $c$ ).<sup>7,29</sup> The correlators  $\langle S_{0,l}^x S_{0,l'}^x \rangle$  and  $\langle S_{\pi,l}^z S_{\pi,l'}^z \rangle$  decay exponentially,<sup>7</sup> because they involve the massive fields. This result also matches the strong-coupling limit. Moreover, the incommensurate wavenumber for the short-ranged correlators is  $\tilde{q} = \pi M$ , which is different from the IC wavenumber for the quasi-long-ranged correlators  $q = 2\pi(M - 1/2)$ . For example, it was found that<sup>7</sup>

$$\langle S_{\pi,l}^z S_{\pi,l'}^z \rangle = \tilde{A}_z (-1)^{l-l'} e^{-|l-l'|/\xi} \frac{\cos[\pi M(l-l')]}{|l-l'|^{1/2+1/4\eta}}, \quad (36)$$

where  $\xi$  is a correlation length for a massive mode and  $\tilde{A}_z$  is a constant.

We have seen that, both in the strong- and weak-coupling limits, the low-energy physics of the two-leg ladder in the gapless regime is in the same universality class as the  $XXZ$  chain in a magnetic field. In particular, the spin correlation functions  $\langle S_{\pi,l}^x S_{\pi,l'}^x \rangle$  and  $\langle S_{0,l}^z S_{0,l'}^z \rangle$  and the local magnetization  $\langle S_{0,l}^z \rangle$  have the same forms as the corresponding functions in the  $XXZ$  chain, but with the shifted wavenumber  $2\pi(M - 1/2)$  and with different values of  $K$ ,  $a$ ,  $b$ , and  $c$ .<sup>30</sup> It is then very natural to postulate that the universality is not restricted to the two limits but holds for any  $j$ . This allows us to use Eqs. (30)–(32) for analyzing the correlation functions in the ladder for any  $j$  and  $M$  ( $0 < M < 1$ ). We can thus determine the TL-liquid parameter  $K$  of the ladder by fitting the numerical data to Eqs. (30)–(32) in the same way as we did for the  $XXZ$  chain. The result is presented in the next subsection. Finally, we may expect that the  $|l - l'|$  dependence of the short-ranged correlators  $\langle S_{0,l}^x S_{0,l'}^x \rangle$  and  $\langle S_{\pi,l}^z S_{\pi,l'}^z \rangle$  obtained in the weak-coupling analysis, such as Eq. (36), should also be valid for any  $j$  and  $M$  ( $0 < M < 1$ ).

## B. Numerical Results

Here we present the result of the DMRG calculation of the two-spin correlations  $\langle S_{\pi,l}^x S_{\pi,l'}^x \rangle$  and  $\langle S_{0,l}^z S_{0,l'}^z \rangle$  and the local magnetization  $\langle S_{0,l}^z \rangle$  in the ladder. Taking  $R$ ,

$a$ ,  $b$ , and  $c$  as free parameters, we fit the data to the formulas (30)–(32) for several values of  $j$  and estimate the  $M$  dependence of  $K = 1/(4\pi R^2)$ . The numerical calculations were performed for the open ladder  $\mathcal{H} + \mathcal{H}'$  of  $L = 100$  rungs (200 sites) for  $j = 10.0, 2.0, 1.0, 0.5$  and  $\Delta = 1.0, 0.5, 0.0$  using the finite-system DMRG method of the improved version. We calculated the two-spin correlations for  $l = r_0 - r/2$  and  $l' = r_0 + r/2$ , where  $r_0 = L/2$  for even  $r$  and  $r_0 = (L + 1)/2$  for odd  $r$ . The maximum value of the kept states  $m$  is 160. From the difference between the data with  $m = 160$  and those with  $m = 120$ , we estimate the numerical error due to the truncation. The estimated errors for  $\langle S_{\pi,l}^x S_{\pi,l'}^x \rangle$ ,  $\langle S_{0,l}^z S_{0,l'}^z \rangle$ , and  $\langle S_l^z \rangle$  are, at largest, of order  $10^{-4}$ ,  $10^{-6}$ , and  $10^{-6}$ , which is almost negligible. In the course of the calculation, we optimized the value of the extra boundary field  $h'$  to minimize the effect of the boundary field.<sup>31</sup> For finite  $j$ , however, the boundary effect cannot be eliminated completely since it can be represented by the form of  $\mathcal{H}'$  only in the strong-coupling limit  $j \gg 1$ . As a result, the two-spin correlation functions and the local magnetization in the open ladder  $\mathcal{H} + \mathcal{H}'$  might deviate from the expected form, Eqs. (30)–(32), near the boundaries. For this reason we used data of smaller range of  $r$  for the fitting than in Sec. II to reduce the unwanted boundary effect. We chose the regions  $10 \leq r \leq 70$ ,  $10 \leq r \leq 80$ ,  $20 \leq r \leq 70$ , and  $20 \leq r \leq 80$  for the fitting of the two-spin correlators and  $10 \leq l \leq 90$  and  $20 \leq l \leq 80$  for the local magnetization. As in Sec. II, we regard the mean and the variance of the fitting parameters obtained for these different ranges of  $r$  and  $l$  as the estimated value and the error of the estimates, respectively. Incidentally, we have also checked for  $(j, M) = (10.0, 0.5)$  that, without the boundary field  $h'$ , the local magnetization  $\langle S_{0,l}^z \rangle$  has the Friedel oscillations induced by the effective boundary field. We found that the oscillations decay algebraically into the bulk with the exponent  $K$ , as expected from the bosonization analysis.<sup>32</sup>

The numerical data of  $\langle S_{\pi,l}^x S_{\pi,l'}^x \rangle$ ,  $\langle S_{0,l}^z S_{0,l'}^z \rangle$ , and  $\langle S_{0,l}^z \rangle$  for  $j = 10.0$  and  $1.0$  with  $\Delta = 1.0$  (Heisenberg case) are shown in Figs. 3 and 4 by open symbols, whose sizes are larger than the truncation error mentioned above. The small solid symbols in the figures are the fits to the DMRG data of the two-spin correlations for  $10 \leq r \leq 80$  and to those of the local magnetization for  $10 \leq l \leq 90$ , respectively. It is clearly seen that the fitting works extremely well for  $j = 10.0$ , confirming the validity of the formulas (30), (31), and (32). Furthermore, the agreement between the numerical data and the fits at  $j = 1.0$  is also quite good except some deviations near the boundary, indicating that the formulas are accurate for the intermediate-coupling regime of  $j$  as well. We note that the quality of the fitting is also good for other values of  $j$  and  $\Delta$  that we have examined. We therefore conclude that the gapless mode of the two-leg ladders is a TL liquid for arbitrary  $j$ , and accordingly, the properties of the strong- and weak-coupling ladders are smoothly

connected.

Next we show in Fig. 5 the  $M$  dependence of  $K$  estimated from the data of  $\langle S_{\pi,l}^x S_{\pi,l'}^x \rangle$  for various  $j$  in both the Heisenberg ( $\Delta = 1.0$ ) and  $XY$  ( $\Delta = 0$ ) cases. In the earlier study<sup>33</sup> the exponent  $\eta$  was obtained for  $j = 5.0$  in the Heisenberg case only. We note that the estimation from  $\langle S_{\pi,l}^x S_{\pi,l'}^x \rangle$  is more reliable than that from  $\langle S_{0,l}^z S_{0,l'}^z \rangle$  or  $\langle S_{0,l}^z \rangle$  as we have seen in the  $XXZ$  chain. Theoretically<sup>7</sup> it is expected that  $K$  should approach the universal value  $K = 1$  when  $M \rightarrow 0$  as well as when  $M \rightarrow 1$ , since the system is equivalent to the dilute limit of hard-core bosons. Although the data for  $M \rightarrow 0$  have large error bars, we may conclude that our results for the Heisenberg case are consistent with the theoretical prediction. Our results for the  $XY$  case show a more subtle feature. At first sight the results for weaker couplings ( $j = 1.0$  and  $0.5$ ) do not seem to approach  $K = 1$  as  $M \rightarrow 0$ . We think, however, that  $K$  changes very rapidly at small  $M$  to approach  $K = 1$ , in view of the data for  $j = 10.0$  and  $2.0$ , which are consistent with the theory. Unfortunately, it is difficult to numerically estimate  $K$  for small  $M$  with high accuracy to resolve this issue.

In the strong-coupling limit  $j \gg 1$ , the ladder system with anisotropy  $\Delta$  is equivalent to the  $S = 1/2$   $XXZ$  chain with anisotropy  $\Delta/2$ , as explained in the previous subsection. Figure 5 clearly shows that the estimated value of  $K$  for  $j = 10.0$  is consistent with the anticipated behavior shown as the dotted curves in both the Heisenberg and  $XY$  cases. As  $j$  decreases,  $K$  increases monotonically for any  $M$  ( $0 < M < 1$ ). Thus,  $K$  is always larger than 1 in the  $XY$  ladder because  $K \rightarrow 1$  for any  $M$  in the large  $j$  limit. In the Heisenberg ladder, on the other hand,  $K$  is smaller than 1 in the strong-coupling limit, as expected from the mapping to the  $XXZ$  chain. Upon decreasing the interchain coupling  $j$ ,  $K$  starts to increase and the  $K$ - $M$  relation changes from a concave curve to a convex one. We note that the similar behavior is observed also in the ladder with  $\Delta = 0.5$ : As  $j$  decreases, the  $K$ - $M$  relation changes from a concave curve at  $j \gg 1$ , corresponding to the behavior of the  $XXZ$  chain with anisotropy  $\Delta/2 = 0.25$ , to a convex one. We thus consider that this behavior of the  $K$ - $M$  curve is an universal feature for  $0 < \Delta \leq 1$ .

The TL-liquid parameter  $K$  determines the long-distance behavior of correlation functions in the thermodynamic limit. For example, the leading term of the correlator  $\langle S_{0,l}^z S_{0,l'}^z \rangle - M^2$  decays as  $\cos[2\pi M(l-l')]/|l-l'|^{2K}$  for  $K < 1$ , while it decays like  $|l-l'|^{-2}$  for  $K > 1$ . Hence, in the ladder with  $0 < \Delta \leq 1$  the leading term of the correlator changes from  $\cos[2\pi M(l-l')]/|l-l'|^{2K}$  to  $|l-l'|^{-2}$  at a critical value  $j_c(M)$  as  $j$  decreases, while in the  $XY$  ladder the leading term is always  $|l-l'|^{-2}$ . On the other hand, the correlator  $\langle S_{\pi,l}^x S_{\pi,l'}^x \rangle$  decays as  $(-1)^{l-l'}/|l-l'|^{1/2K}$  in the whole range of  $K$  covered in Figs. 5 (a) and 5 (b). The temperature dependence of the spin-lattice relaxation rate  $1/T_1$  in NMR experi-

ments is directly related to the TL-liquid parameter  $K$  through the decay exponent of the most slowly decaying correlation.<sup>5</sup> From the behavior of  $K$ - $M$  relation obtained above, we find that the correlator  $\langle S_{\pi,l}^x S_{\pi,l'}^x \rangle$  decays most slowly for any  $j$ ,  $M$ , and  $0 \leq \Delta \leq 1$ . We therefore conclude that at low temperatures the relaxation rate of the ladder in the gapless regime always shows a power-law divergence  $1/T_1 \propto T^{-1+(1/2K)}$ .

Figure 6 shows the numerical result of  $\langle S_{\pi,l}^z S_{\pi,l'}^z \rangle$  for the Heisenberg ladder at  $j = 0.5$ . It exhibits exponentially decaying oscillatory behavior. From the period  $\lambda$  of oscillations, we obtain the IC wavenumber  $\tilde{q} = 2\pi/\lambda$  as a function of  $M$ ; see the inset figure. The result confirms the theoretical prediction  $\tilde{q} = \pi M$ . This IC wavenumber  $\tilde{q}$  tells us that the massive magnon dispersion has a minimum excitation energy at<sup>7</sup>  $q = \pi - \tilde{q} = \pi(1-M)$ . Accordingly, the dynamical spin structure factor  $S_{\pi}^{zz}(q, \omega)$  should have a power-law divergence along the energy dispersion which is roughly shifted by  $\pi M$  from that of the triplet magnon dispersion in the absence of the magnetic field. It would be interesting if this feature is observed by inelastic neutron scattering experiments.

#### IV. CONCLUSIONS

In this paper we have studied the ground-state spin correlations in the gapless IC regime of the  $S = 1/2$   $XXZ$  chain and the two-leg AF ladder in a magnetic field. We have used the  $S = 1/2$   $XXZ$  chain as a first test ground to apply the method we developed in our previous work: We numerically computed the two-spin correlation functions and the local magnetization by the DMRG method and fit the results to functions which are obtained using the bosonization technique. The fitting parameters are the TL-liquid parameter  $K$  and the amplitudes of bosonic operators. We found good agreement between  $K$  estimated from the fitting and  $K$  calculated from the Bethe ansatz. As a byproduct we obtained the amplitudes of the dominant terms in  $\langle S_l^x S_{l'}^x \rangle$  and  $\langle S_l^z S_{l'}^z \rangle$ .

We have applied the same technique to the two-leg AF ladder in the gapless IC regime. It has been known that in both the strong- and weak-coupling limits the low-energy excitations in the ladder are regarded as a TL liquid like the  $XXZ$  chain in a field. We fit our DMRG data of the two-spin correlation functions and the local magnetization of the ladder to the same bosonization formulas we used in the analysis of the  $XXZ$  chain. The fitting worked very well not only in the strong- and weak-coupling limits but for broad range of the interchain coupling strength  $j$ . We thereby confirmed that the low-energy gapless excitations are indeed described as the TL liquid for any  $j$  and the properties of the strong- and weak-coupling ladders are smoothly connected. For several values of  $j$ , we have determined  $K$ , which shows non-trivial  $j$  and  $M$  dependences (Fig. 5). It turned out that, for any  $M$  ( $0 < M < 1$ ),  $K$  is a monotonically decreasing

function of  $j$ . In the ladder with anisotropy  $0 < \Delta \leq 1$  the  $K$ - $M$  relation changes from a concave curve at  $j \gg 1$  to a convex one as  $j$  decreases, while in the  $XY$  ladder ( $\Delta = 0$ ) it changes from a line  $K = 1$  at  $j \gg 1$  to a convex curve. We also found that the spin-lattice relaxation rate in NMR measurement shows a power-law divergence  $1/T_1 \propto T^{-1+(1/2K)}$  at low temperature for any  $j$ .

## ACKNOWLEDGMENTS

Numerical computations were performed at the Yukawa Institute Computing Facility. The work of AF was in part supported by Grant-in-Aid for Scientific Research on Priority Areas (A) from the Ministry of Education, Science, Sports and Culture (No. 12046238) and by Grant-in-Aid for Scientific Research from the Japan Society for the Promotion of Science (No. 11740199).

## APPENDIX: DERIVATION OF CORRELATORS

We briefly explain the derivation of Eqs. (11) and (12). As is always the case with the bosonization, we need to introduce a short-distance cutoff to obtain finite results. The lattice spacing in the original Hamiltonian serves as the natural cutoff scale.

When we use Eqs. (3) and (4) with the mode expansions (7) and (8), we encounter the summation

$$\sum_{n=1}^{\infty} \frac{1}{n} \left[ 1 - \cos \left( \frac{\pi n l}{L+1} \right) \right], \quad (\text{A1})$$

which is formally divergent. We regularize it by inserting an exponential factor  $e^{-\pi n/(L+1)}$ :

$$\sum_{n=1}^{\infty} \frac{1}{n} e^{-\pi n/(L+1)} \left[ 1 - \cos \left( \frac{\pi n l}{L+1} \right) \right] = \ln[f(l)], \quad (\text{A2})$$

where  $f(l) \equiv f_1(l)$  defined in Eq. (15). We note that Eq. (A2) is a very good approximation except near the points where  $f_1(l)$  is divergent. Taking derivatives with respect to  $l$ , we obtain

$$\sum_{n=1}^{\infty} e^{-\pi n/(L+1)} \sin \left( \frac{\pi n l}{L+1} \right) = \frac{1}{2} \cot \left( \frac{\pi l}{2(L+1)} \right) \quad (\text{A3})$$

and

$$\sum_{n=1}^{\infty} n e^{-\pi n/(L+1)} \cos \left( \frac{\pi n l}{L+1} \right) = -\frac{1}{4 \sin^2 \left( \frac{\pi l}{2(L+1)} \right)}. \quad (\text{A4})$$

Another point to note is that for  $\varepsilon_i = \pm 1$

$$\begin{aligned} \langle e^{i2\pi R \varepsilon_1 \tilde{\phi}(l)} e^{i2\pi R \varepsilon_2 \tilde{\phi}(l')} \rangle &\propto \int_0^{1/R} R e^{i2\pi R(\varepsilon_1 + \varepsilon_2) \tilde{\phi}_0} d\tilde{\phi}_0 \\ &\propto \delta_{\varepsilon_1 + \varepsilon_2, 0}. \end{aligned} \quad (\text{A5})$$

With the above-mentioned formulas, it is straightforward to obtain

$$\begin{aligned} \langle \cos[2\pi R \tilde{\phi}(l)] \cos[2\pi R \tilde{\phi}(l')] \rangle &= \frac{[f(2l)f(2l')]^{\eta/2}}{2[f(l-l')f(l+l')]^{\eta}}, \\ \langle e^{i2\pi R \varepsilon_1 \tilde{\phi}(l)} e^{-i2\pi R \varepsilon_1 \tilde{\phi}(l')} e^{i\varepsilon_2 \phi(l')/R} \rangle \\ &= i\varepsilon_1 \varepsilon_2 e^{iq\varepsilon_2 l'} \frac{\text{sgn}(l-l')[f(2l)f(2l')]^{\eta/2}}{[f(l-l')f(l+l')]^{\eta} [f(2l')]^{1/2\eta}}, \\ \langle e^{i2\pi R \varepsilon_0 \tilde{\phi}(l)} e^{i\varepsilon_1 \phi(l)/R} e^{-i2\pi R \varepsilon_0 \tilde{\phi}(l')} e^{i\varepsilon_2 \phi(l')/R} \rangle \\ &= -\varepsilon_1 \varepsilon_2 e^{iq(\varepsilon_1 l + \varepsilon_2 l')} \frac{[f(2l)f(2l')]^{\eta/2-1/2\eta}}{[f(l-l')f(l+l')]^{\eta}} \left( \frac{f(l-l')}{f(l+l')} \right)^{\varepsilon_1 \varepsilon_2 / \eta}, \\ \left\langle \frac{d\phi}{dl} \frac{d\phi}{dl'} \right\rangle &= -\frac{1}{2\pi} \left( \frac{1}{f_2(l-l')} + \frac{1}{f_2(l+l')} \right) + \left( \frac{q}{2\pi} \right)^2, \\ \left\langle \left( \frac{d\phi}{dl} - \frac{q}{2\pi} \right) \sin \frac{\phi(l')}{R} \right\rangle &= \frac{\cos(q l')}{2\pi R} \frac{g(l+l') - g(l-l')}{[f(2l')]^{1/2\eta}}, \\ \langle e^{i\varepsilon_1 \phi(l)/R} e^{i\varepsilon_2 \phi(l')/R} \rangle &= \frac{e^{iq(\varepsilon_1 l + \varepsilon_2 l')}}{[f(2l)f(2l')]^{1/2\eta}} \left( \frac{f(l-l')}{f(l+l')} \right)^{\varepsilon_1 \varepsilon_2 / \eta}. \end{aligned}$$

<sup>1</sup> For a review, see, *e.g.*, E. Dagotto and T.M. Rice, *Science* **271**, 618 (1996).

<sup>2</sup> P. W. Anderson, *Science* **235**, 1196 (1987).

<sup>3</sup> M. Azuma, Z. Hiroi, M. Takano, K. Ishida, and Y. Kitaoka, *Phys. Rev. Lett.* **73**, 3463 (1994).

<sup>4</sup> G. Chaboussant, P.A. Crowell, L.P. Lévy, O. Piovesana, A. Madouri, and D. Mailly, *Phys. Rev. B* **55**, 3046 (1997); G. Chaboussant, Y. Fagot-Revurat, M.-H. Julien, M.E. Hanson, C. Berthier, M. Horvatić, L.P. Lévy, and O. Piovesana, *Phys. Rev. Lett.* **80**, 2713 (1998).

<sup>5</sup> R. Chitra and T. Giamarchi, *Phys. Rev. B* **55**, 5816 (1997). They concluded incorrectly that the incommensurate correlations in a spin ladder decay exponentially and the power-law components appear only at  $q = 0$  and  $\pi$ . This was corrected in Refs. 7 and 6.

<sup>6</sup> T. Giamarchi and A.M. Tsvelik, *Phys. Rev. B* **59**, 11398 (1999).

<sup>7</sup> A. Furusaki and S.C. Zhang, *Phys. Rev. B* **60**, 1175 (1999).

<sup>8</sup> T. Hikihara and A. Furusaki, *Phys. Rev. B* **58**, R583 (1998).

<sup>9</sup> S.R. White, *Phys. Rev. Lett.* **69**, 2863 (1992).

<sup>10</sup> S.R. White, *Phys. Rev. B* **48**, 10345 (1993).

<sup>11</sup> C.N. Yang and C.P. Yang, *Phys. Rev.* **150**, 321 (1966).

<sup>12</sup> F.D.M. Haldane, *Phys. Rev. Lett.* **45**, 1358 (1980).

<sup>13</sup> F. Woynarovich, H.-P. Eckle, and T.T. Truong, *J. Phys. A: Math. Gen.* **22**, 4027 (1989).

<sup>14</sup> S. Eggert and I. Affleck, *Phys. Rev. B* **46**, 10866 (1992).



- <sup>15</sup> M. Fabrizio and A.O. Gogolin, Phys. Rev. B **51**, 17827 (1995).  
<sup>16</sup> R. Egger and H. Grabert, Phys. Rev. Lett. **75**, 3505 (1995).  
<sup>17</sup> S. Eggert, H. Johannesson, and A. Mattsson, Phys. Rev. Lett. **76**, 1505 (1996).  
<sup>18</sup> G. Bedürftig, B. Brendel, H. Frahm, and R.M. Noack, Phys. Rev. B **58**, 10225 (1998).  
<sup>19</sup> N.M. Bogoliubov, A.G. Izergin, and V.E. Korepin, Nucl. Phys. B **275**, 687 (1986).  
<sup>20</sup> D.C. Cabra, A. Honecker, and P. Pujol, Phys. Rev. B **58**, 6241 (1998).  
<sup>21</sup> S.R. White, Phys. Rev. Lett. **77**, 3633 (1996).  
<sup>22</sup> S. Lukyanov and A. Zamolodchikov, Nucl. Phys. B **493**, 571 (1997).  
<sup>23</sup> S. Lukyanov, Phys. Rev. B **59**, 11163 (1999).  
<sup>24</sup> We are not sure about the accuracy of our estimates for the amplitude  $\hat{A}_x$  of the subleading term, and thereby we do not show them here.  
<sup>25</sup> The estimates of  $A_z$  for small  $M > 0$  shown in Table I (b) do not seem to approach smoothly the exact value at

- $M_{\text{ch}} = 0$  as  $M_{\text{ch}} \rightarrow 0$ . We do not know exactly the reason why this happens. This might be due to the same reason as the one for the deviation of  $K$  estimated from  $\langle S_i^z \rangle$  mentioned in the text.  
<sup>26</sup> F. Mila, Eur. Phys. J. B **6**, 201 (1998).  
<sup>27</sup> K. Totsuka, Phys. Rev. B **57**, 3454 (1998).  
<sup>28</sup> D.G. Shelton, A.A. Nersisyan, and A.M. Tsvelik, Phys. Rev. B **53**, 8521 (1996).  
<sup>29</sup> We note that the notation has changed from Ref. 7. The parameter  $\eta$  in the present paper is equal to the inverse of the  $\eta$  used in Ref. 7.  
<sup>30</sup> In the strong-coupling limit, the parameters  $K$ ,  $a$ ,  $b$ , and  $c$  in the ladder with the anisotropy  $\Delta$  are related to those in the  $XXZ$  chain with the anisotropy  $\Delta/2$ ; see Eqs. (30)-(33).  
<sup>31</sup> To be more concrete, we optimized the value of  $h'$  to minimize the deviation of  $\langle S_{0,l}^z \rangle$  for  $M = 1/2$  from the constant value,  $1/2$ ; see Eq. (32).  
<sup>32</sup> I. Affleck, J. Phys. A: Math. Gen. **31**, 2761 (1998).  
<sup>33</sup> M. Usami and S. Suga, Phys. Rev. B **58**, 14401 (1998).

TABLE I. The correlation amplitudes; (a)  $A_x = c^2/2$  estimated from the data of  $\langle S_i^x S_j^x \rangle$ ; (b)  $A_z = a^2/2$  estimated from the data of  $\langle S_i^z \rangle$ . The figures in parentheses indicate the error bar on the last quoted digits. The error bars of  $A_z$  for  $\Delta = 0$  and  $0.05 \leq M \leq 0.45$  are smaller than  $10^{-5}$ . The exact values for  $M_{\text{ch}} = 0$  given by Eqs. (20) and (21) are also listed.

(a) $A_x$										
$M_{\text{ch}}$	0	0.05	0.10	0.15	0.20	0.25	0.30	0.35	0.40	0.45
$\Delta = 0.0$	0.14709	0.14626(1)	0.14364(6)	0.1390(1)	0.13262(1)	0.12410(6)	0.1132(3)	0.0993(7)	0.081(2)	0.0594(7)
$\Delta = 0.1$	0.14451	0.14369(7)	0.1413(1)	0.1371(1)	0.13101(7)	0.12293(2)	0.1125(3)	0.0991(7)	0.081(2)	0.0597(7)
$\Delta = 0.2$	0.14187	0.1408(4)	0.1390(2)	0.1351(2)	0.1294(1)	0.12174(5)	0.1111(7)	0.0988(6)	0.081(2)	0.0600(7)
$\Delta = 0.3$	0.13921	0.1384(3)	0.1366(3)	0.1330(3)	0.1278(2)	0.12053(9)	0.1111(2)	0.0985(6)	0.081(2)	0.0601(7)
$\Delta = 0.4$	0.13656	0.1358(3)	0.1342(4)	0.1310(3)	0.1261(3)	0.1193(1)	0.1104(1)	0.0982(6)	0.081(2)	0.0603(7)
$\Delta = 0.5$	0.13400	0.1332(4)	0.1318(5)	0.1289(4)	0.1245(3)	0.1182(2)	0.10973(9)	0.0979(5)	0.081(2)	0.0605(7)
$\Delta = 0.6$	0.13164	0.1310(5)	0.1294(6)	0.1268(5)	0.1229(4)	0.1170(2)	0.10905(7)	0.0976(5)	0.081(2)	0.0606(7)
$\Delta = 0.7$	0.12973	0.1281(6)	0.1270(7)	0.1248(5)	0.1213(4)	0.1159(3)	0.10839(6)	0.0973(5)	0.081(2)	0.0607(7)
$\Delta = 0.8$	0.12896	0.1257(8)	0.1247(8)	0.1227(6)	0.1197(5)	0.1148(3)	0.10775(7)	0.0970(5)	0.081(1)	0.0609(7)
$\Delta = 0.9$	0.13214	0.1233(9)	0.1223(9)	0.1207(7)	0.1182(6)	0.1137(3)	0.10714(8)	0.0967(4)	0.081(1)	0.0610(8)
$\Delta = 1.0$		0.121(1)	0.120(1)	0.1188(8)	0.1177(9)	0.1127(4)	0.1065(1)	0.0958(6)	0.081(1)	0.0610(8)
(b) $A_z$										
$M_{\text{ch}}$	0	0.05	0.10	0.15	0.20	0.25	0.30	0.35	0.40	0.45
$\Delta = 0.0$	0.05066	0.05066	0.05066	0.05066	0.05066	0.05066	0.05066	0.05066	0.05066	0.05066
$\Delta = 0.1$	0.05929	0.0599(7)	0.0581(3)	0.0567(6)	0.0544(1)	0.0537(7)	0.0513(6)	0.0516(6)	0.049(1)	0.0510(8)
$\Delta = 0.2$	0.06891	0.071(1)	0.0662(6)	0.063(1)	0.0580(2)	0.056(1)	0.052(1)	0.052(1)	0.048(2)	0.051(1)
$\Delta = 0.3$	0.07978	0.083(2)	0.0748(7)	0.069(1)	0.0614(4)	0.059(1)	0.052(1)	0.053(1)	0.048(2)	0.052(2)
$\Delta = 0.4$	0.09231	0.097(3)	0.0838(6)	0.075(1)	0.0645(6)	0.060(1)	0.053(2)	0.053(2)	0.047(3)	0.052(2)
$\Delta = 0.5$	0.10713	0.113(5)	0.093(4)	0.080(1)	0.0674(8)	0.062(2)	0.053(2)	0.053(2)	0.046(3)	0.052(3)
$\Delta = 0.6$	0.12539	0.132(6)	0.10263(5)	0.0854(9)	0.070(1)	0.063(2)	0.054(2)	0.053(2)	0.046(3)	0.052(3)
$\Delta = 0.7$	0.14930	0.153(8)	0.1121(5)	0.0903(4)	0.072(1)	0.065(2)	0.054(2)	0.053(2)	0.045(4)	0.052(3)
$\Delta = 0.8$	0.18414	0.176(10)	0.121(1)	0.09486(6)	0.074(2)	0.066(2)	0.054(2)	0.054(2)	0.045(4)	0.052(4)
$\Delta = 0.9$	0.24844	0.20(1)	0.131(2)	0.0990(7)	0.076(2)	0.067(1)	0.054(2)	0.054(2)	0.047(4)	0.052(4)
$\Delta = 1.0$		0.23(1)	0.139(3)	0.103(1)	0.078(2)	0.067(1)	0.054(3)	0.054(2)	0.044(4)	0.052(4)

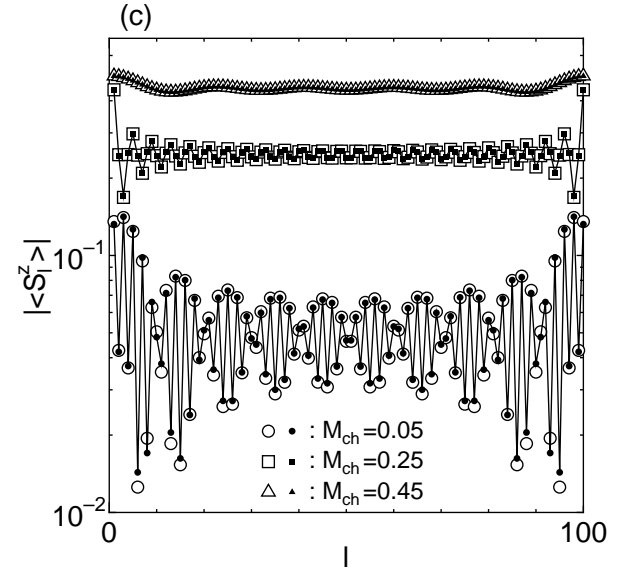
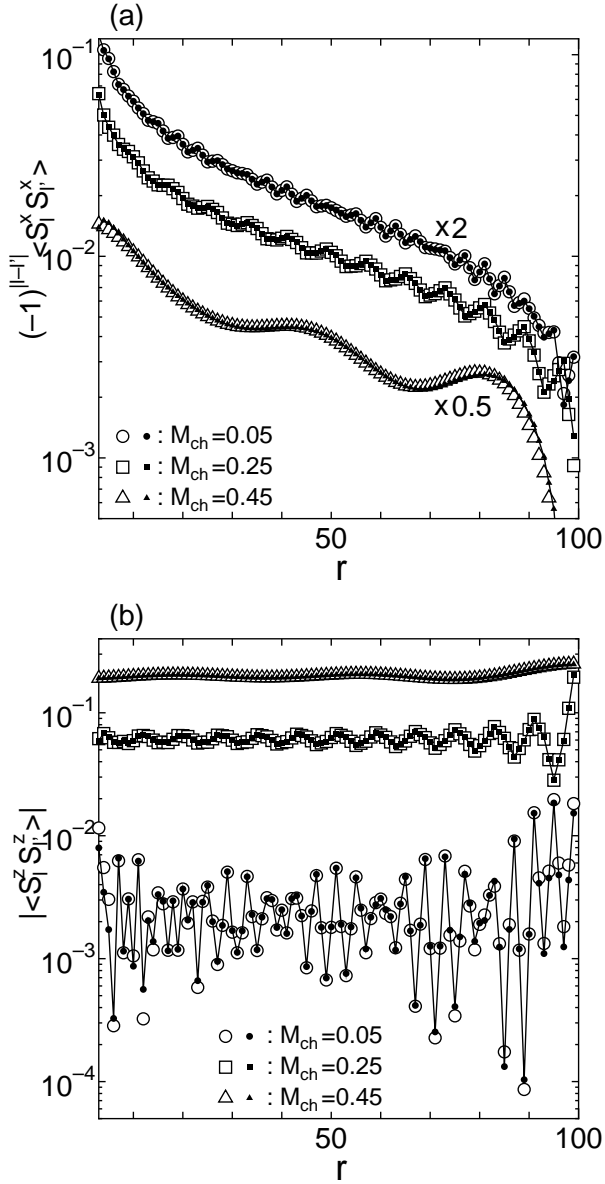


FIG. 1. (a)  $(-1)^{|l-l'|} \langle S_l^x S_{l'}^x \rangle$  versus  $r = |l-l'|$ , (b)  $|\langle S_l^z S_{l'}^z \rangle|$  versus  $r$ , (c)  $\langle S_l^z \rangle$  versus  $l$  for  $\Delta = 0.5$  and  $M_{\text{ch}} = 0.05, 0.25$ , and  $0.45$ . The open symbols are the DMRG data and small solid symbols are the fits. The numerical errors of the DMRG data are smaller than the size of the open symbols. The data of  $(-1)^{|l-l'|} \langle S_l^x S_{l'}^x \rangle$  for  $M_{\text{ch}} = 0.05$  and  $0.45$  in figure (a) are multiplied by a factor of 2 and 0.5, respectively.

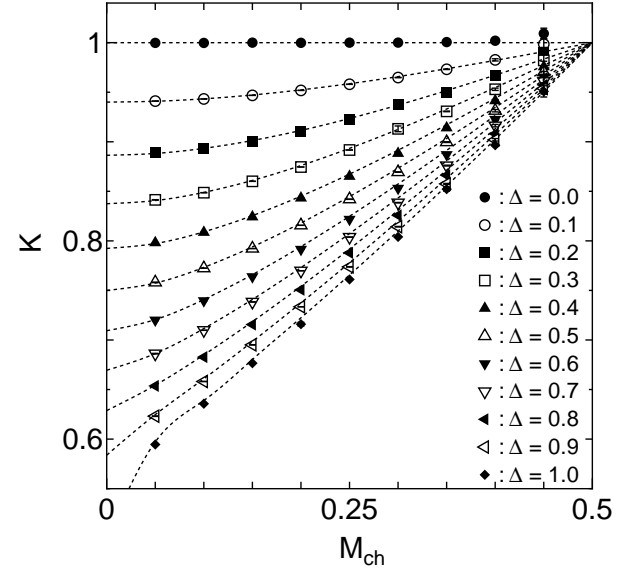


FIG. 2. The results of  $K = 1/(4\pi R^2)$  estimated from the fitting of  $\langle S_l^x S_{l'}^x \rangle$  for  $0 \leq \Delta \leq 1.0$ . The dotted curves represent the exact values obtained from Bethe ansatz.

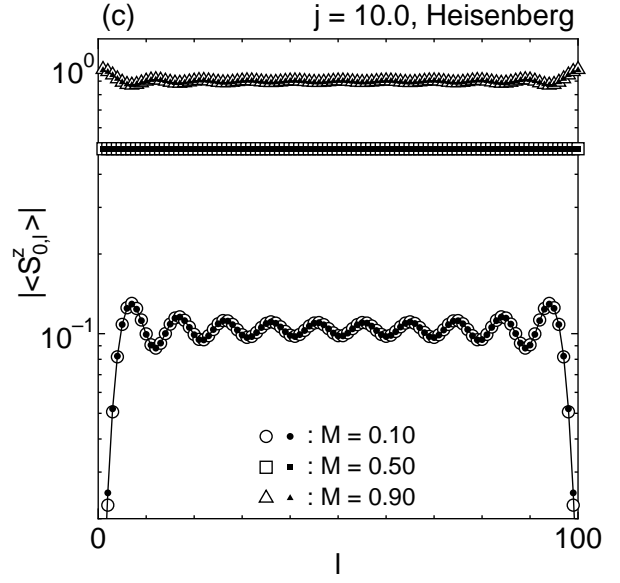
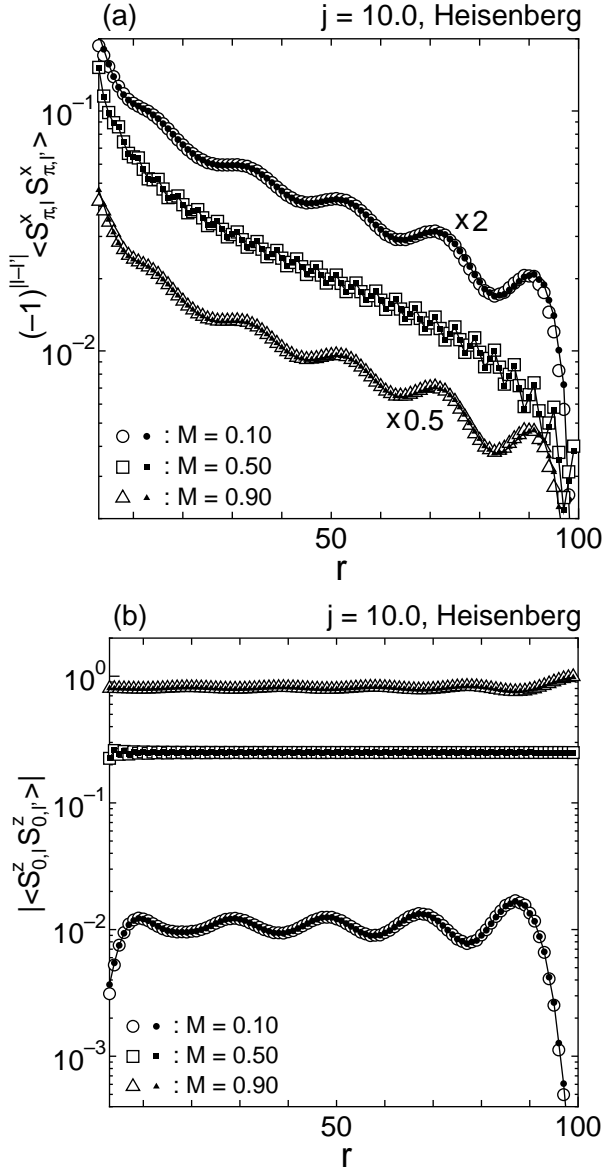
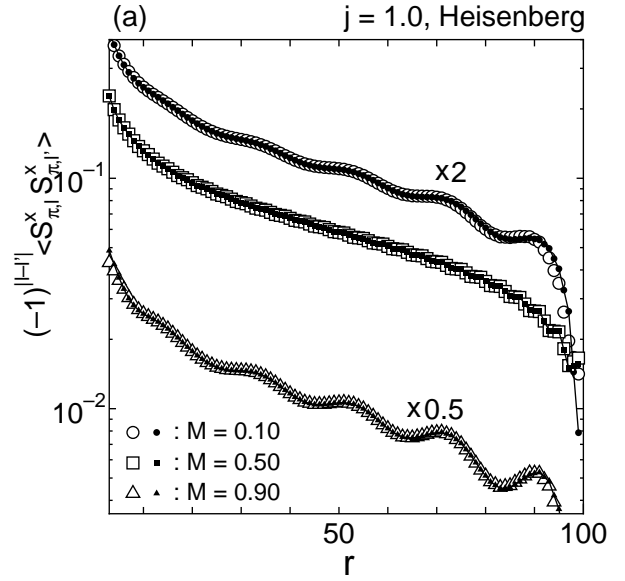


FIG. 3. (a)  $(-1)^{|l-l'|} \langle S_{\pi,l}^x S_{\pi,l'}^x \rangle$  versus  $r = |l - l'|$ , (b)  $|\langle S_{0,l}^z S_{0,l'}^z \rangle|$  versus  $r$ , (c)  $\langle S_{0,l}^z \rangle$  versus  $l$  for  $j = 10.0$  and the Heisenberg case ( $\Delta = 1.0$ ). The open symbols are the DMRG data and small solid symbols are the fits. The numerical errors of the DMRG data are smaller than the size of the open symbols. The data of  $(-1)^{|l-l'|} \langle S_{\pi,l}^x S_{\pi,l'}^x \rangle$  for  $M = 0.10$  and  $0.90$  in figure (a) are multiplied by a factor of 2 and 0.5, respectively.



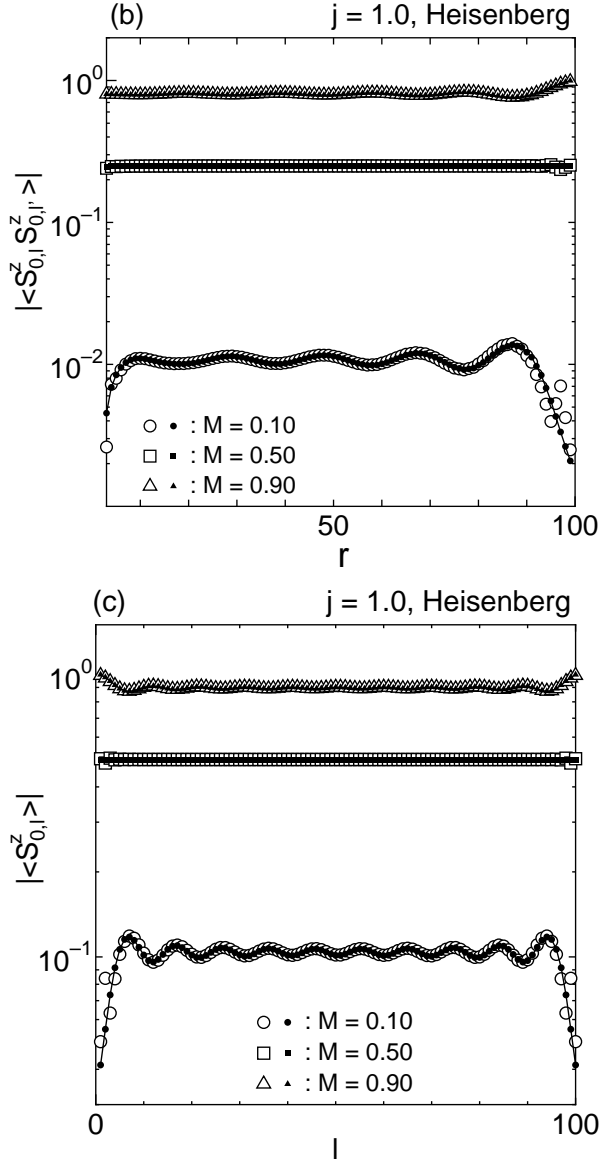


FIG. 4. (a)  $(-1)^{|l-l'|} \langle S_{\pi,l}^x S_{\pi,l'}^x \rangle$  versus  $r = |l - l'|$ , (b)  $|\langle S_{0,l}^z S_{0,l'}^z \rangle|$  versus  $r$ , (c)  $\langle S_{0,l}^z \rangle$  versus  $l$  for  $j = 1.0$  and the Heisenberg case ( $\Delta = 1.0$ ). The open symbols are the DMRG data and small solid symbols are the fitting results. The numerical errors of the DMRG data are smaller than the size of the open symbols. The data of  $(-1)^{|l-l'|} \langle S_{\pi,l}^x S_{\pi,l'}^x \rangle$  for  $M = 0.10$  and  $0.90$  in figure (a) are multiplied by a factor of 2 and 0.5, respectively.

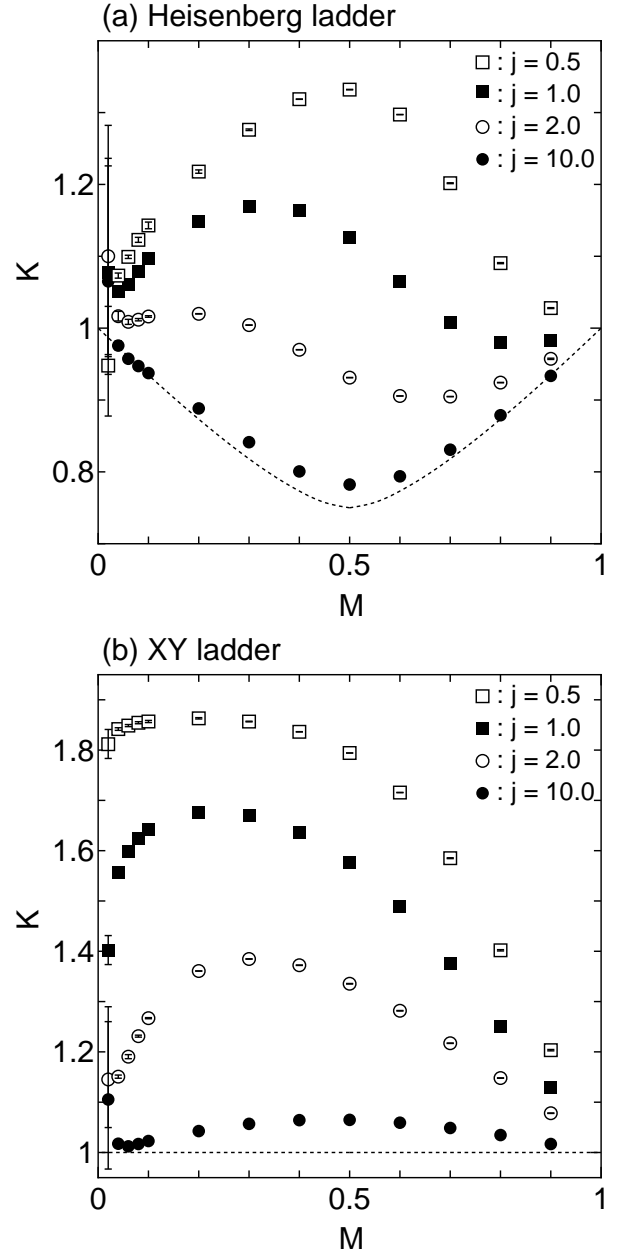


FIG. 5. The TL-liquid parameter  $K = 1/(4\pi R^2)$  estimated from the fitting of  $\langle S_{\pi,l}^x S_{\pi,l'}^x \rangle$  for  $j = 10.0, 2.0, 1.0, 0.5$  and for (a) the Heisenberg ladder ( $\Delta = 1.0$ ) and (b) the XY ladder ( $\Delta = 0$ ). The dotted curves represent the exact values of the  $S = 1/2$  XXZ chain with the anisotropy  $\Delta/2$ .

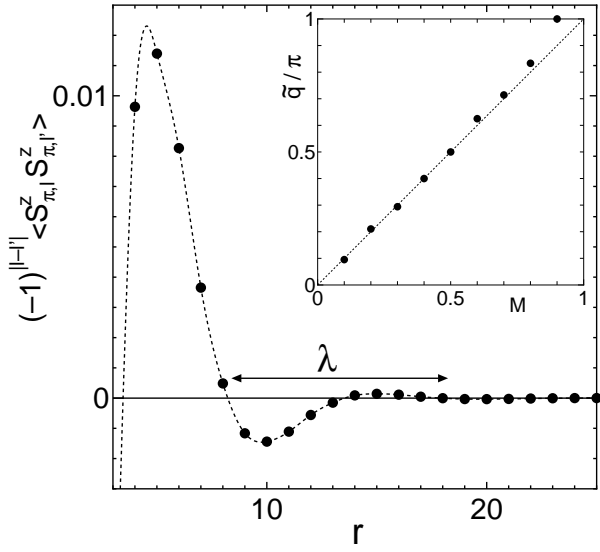


FIG. 6. The correlation function  $(-1)^{|l-l'|} \langle S_{\pi,l}^z S_{\pi,l'}^z \rangle$  in the Heisenberg ladder at  $j = 0.5$  and  $M = 0.2$ . The dotted curve is a guide to the eye. Inset: The  $M$  dependence of the IC wavenumber  $\tilde{q}$  of  $\langle S_{\pi,l}^z S_{\pi,l'}^z \rangle$  in the Heisenberg ladder with  $j = 0.5$ . The dotted line represents the theoretical prediction  $\tilde{q}/\pi = M$ .